

Modeling of Self-Excited Isolated Permanent Magnet Induction Generator Using Iterative Numerical Method

Mostafa R. Mohamed, Karam M. Abdel-Latif^a and Mahmoud R. Ahmed

Department of Electrical Machine and Power Engineering, Faculty of Engineering-Helwan University at Helwan - Egypt

Abstract. Self-Excited Permanent Magnet Induction Generator (PMIG) is commonly used in wind energy generation systems. The difficulty of Self-Excited Permanent Magnet Induction Generator (SEPMIG) modeling is the circuit parameters of the generator vary at each load conditions due to the a change in the frequency and stator voltage. The paper introduces a new modeling for SEPMIG using Gauss-sidle relaxation method. The SEPMIG characteristics using the proposed method are studied at different load conditions according to the wind speed variation, load impedance changes and different shunted capacitor values. The system modeling is investigated due to the magnetizing current variation, the efficiency variation, the power variation and power factor variation. The proposed modeling system satisfies high degree of simplicity and accuracy.

1 Introduction

Permanent Magnet Induction Generator (PMIG) is a new type of induction generator that has a stator equipped with a three phase-winding and two rotors mounted on the machine rotor shaft. The outer rotor has squirrel-cage-windings while the inner free rotor is a Permanent Magnet (PM). The outer squirrel- cage rotor rotates at an angular speed faster than that of the rotating field generated by the generator stator current while the inner PM rotor is free to rotate on the same angular speed of the stator magnetic field. The induced stator voltage due to the PM is compensating the reactive stator current and improves the generator power factor [1]-[5]. The PMIG equivalent circuit is similar to the conventional induction generator equivalent circuit. As many papers mentioned [1], [3] and [5] the flux produced by the internal PM rotor can be modeled as internal voltage source (E_{pm}) in series with the magnetizing reactance as shown in Figure 1. This paper introduces the PMIG model as an isolated unit in wind energy system so this machine is called Self- excited Permanent Magnet Induction Generator (SEPMIG). The PMIG obtains the necessary reactive power (Q) for initiating the magnetic flux in the air-gap from its connection to the grid. In case of SEPMIG there is no connection to the grid so the machine received the necessary reactive power by connecting its terminals with shunt capacitor as shown in Figure 2.

^a Corresponding author : Karam106@yahoo.com

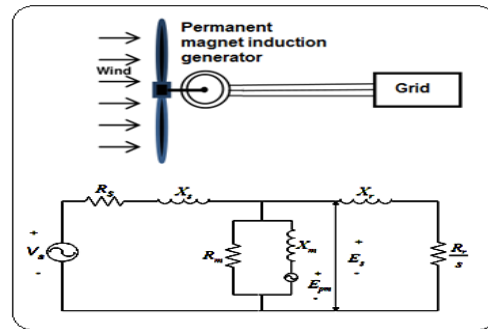


Figure 1. PMIG Equivalent Circuit Connected to Grid [5].

The rest of the paper is organized as follows; The SEPMIG proposed model is given in Section 2, the computational procedure of the proposed model is given in Section 3, case study and the performance results are illustrated in Section 4, and the conclusion is presented in Section 5.

2 Proposed Mathematical Model of SEPMIG

In SEPMIG modeling methods, the terminal machine voltage and generated stator frequency are varying with the operating load conditions. The difficulty of PMSEIG modeling is that all the circuit parameters shown in Figure 2 of the generator vary according to the load condition changes due to the changes in frequency and stator voltage. The proposed model will produce a solution to overcome these difficulties through the following modifications.

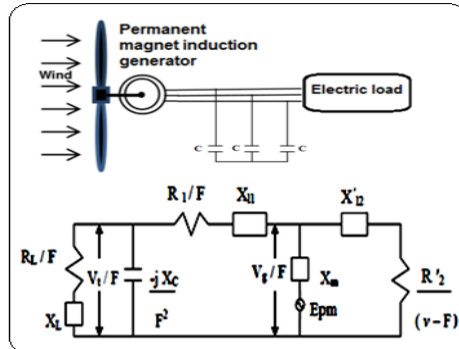


Figure 2. SEPMIG in Wind Energy System [6].

Step:1

The parameters of the equivalent circuit of the SEPMIG are presented in per-unit value based on stator frequency (F).

Step: 2

Appling a Gauss- Sidle iterative solution on SEPMIG to determine the machine parameters such as the magnetizing reactance, stator frequency and induced air gap voltage under specified machine load conditions.

Step: 3

Determine the SEPMIG performance using the machine parameters given in step 2.

The per-unit single phase equivalent circuit of SEPMIG is shown in Figure 3. The parameters are expressed in per unit by taking the line Frequency (F) asbase value.

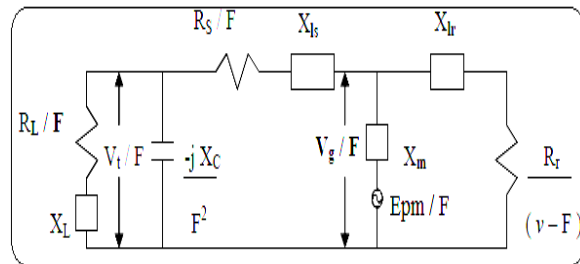


Figure 3. Per Phase SEPMIG Equivalent Circuit.

In this circuit the loading type of SEPMIG are considered as static resistive-inductive load connected in parallel with the shunt capacitor C sh. In this model the core resistance was neglected with respect to shunt magnetizing reactance. The stator resistance and leakage reactance per phase are R_1 and X_{l1} respectively while the rotor resistance and leakage reactance per phase are R'_2 and X'_{l2} respectively.

2.1 Proposed Model Equations

Based on the concept of assuming the linearity of the machine parameters except its magnetizing inductance [7] and [8], the nodal current equation for the single phase equivalent circuit shown in Figure 3 under the steady state operation, will lead to the following equation.

$$I_s + I_r + I_m = 0 \quad (1)$$

where I_s , I_r and I_m are defined as stator current, rotor current and magnetizing current respectively. From the equivalent circuit given in Figure 3, the different currents are obtained as follows:

$$I_s = \frac{V_g/F}{(R_1/F + jX_1) + ((R_L/F + jX_L) // (jX_C/F^2))} \quad (2)$$

$$I_r = \frac{V_g/F}{R'_2/(v-F) + jX'_2} \quad (3)$$

$$I_m = I_s + I_r \quad (4)$$

where V_g , R_L , X_L , F and X_C are defined as the induced air gap voltage, load resistance, load leakage reactance, Per unit frequency with respect to the line frequency and shunt capacitance respectively.

The induced air gap voltage across the magnetizing branch (V_g) and the terminal voltage (V_t) are calculated using equations (5& 6) as follows.

$$\frac{V_g}{F} = E_{pm} + jI_m X_m \quad (5)$$

$$V_t = V_g - I_s \left(\frac{R_s}{F} + jX_s \right) \quad (6)$$

where E_{pm} is the internal armature induced voltage. As the currents of the generator under the steady state condition must be not equal zero, the magnetizing current can be obtained from equation (7) as.

$$I_m = -\frac{E_{pm}}{Z_{eq} + jX_m} \quad (7)$$

where Z_{eq} is the equivalent impedance of SEPMIG that obtained using equation (8)

$$Z_{eq} = \frac{Z_s Z_r}{Z_s + Z_r} \quad (8)$$

$$Z_r = \frac{r'_2 + jX'_{l2}(v-F)}{(v-F)} \quad (9)$$

$$Z_s = \frac{\frac{X_C X_l}{F^2} + \frac{r_1 R_L}{F^2} + \frac{X_{l1} X_C}{F^2} - X_{l1} X_L + j(\frac{X_{l1} R_L}{F} + \frac{r_1 X_L}{F} - \frac{r_1 X_C}{F^3} - \frac{X_C R_L}{F^3})}{\frac{R_L}{F} + j(X_L - \frac{X_C}{F^2})} \quad (10)$$

where Z_s and Z_r are the stator and rotor equivalent impedances respectively.

The solution of equation (5) leads to develop a 5th order polynomial expressed in terms of frequency (F) as expressed in equation (11).

$$A_6 F^5 + A_5 F^4 + A_4 F^3 + A_3 F^{25} + A_2 F + A_1 = 0 \quad (11)$$

where (A1- A6) represent the Polynomial Coefficients, The function of F, V_g , E_{pm} , X_{m12} , S (the machine slip), and the machine parameters. The polynomial equation obtained from equation (11) will be solved using the iterative solution based on Gauss-Sidle relaxation Method.

3 The Computational Procedure

The iterative solution is based on the Gauss-sidle relaxation technique to solve the polynomial equation for the unknown F by assuming the value X_{m12} . The initial values of X_{m12} are reassigned carefully to reduce the number of iteration required to converge the solution. The induced armature voltage E_{pm} is considered as a constant value equal to the system reference voltage. The solution is used to predict a convergent value for the V_g and to be matched with the values "F" and " X_{m12} ". The full performance of SEPMIG is obtained by solving the equivalent circuit taking into consideration the predicted matched values of X_{m12} , F, and V_g . The computational procedure of the proposed model could be summarized in the flowchart shown in Figure4.

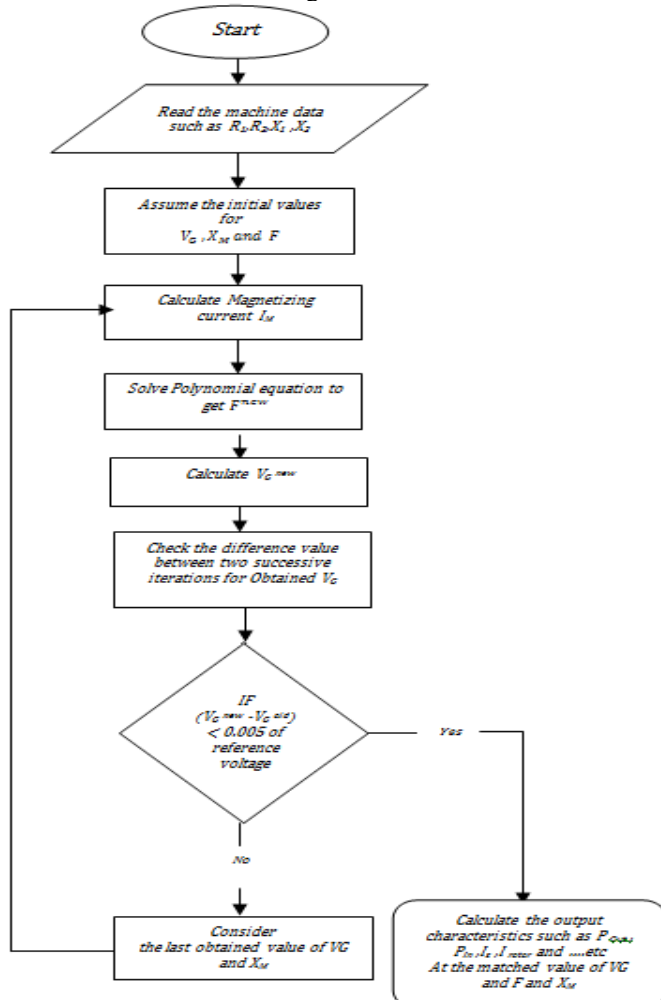


Figure 4. Computational Procedure Flowchart

4 The Estimated Initial Value of the Magnetizing Reactance

The initial values of X_{m12} would be assigned carefully to reduce the number of iterations required to converge the solution. The linear value of X_{m12} is 167Ω and the full parameters of the IG used are given in Table1. The proposed PMSEIG would be needed to modify the machine rotor [1] by considering a PM of approximately is 6 mm thickness placed on the surface of the inner rotor. Both outer and inner rotors are separated by air-gap of 1 mm thickness. Consequently, the linear value of X_{m12} is reduced to 20% approximately 32Ω . However, the difficulty of assigning initial values for X_{m12} is due to the effect of the machine core saturation in addition to the effect of the wind-speed variation as shown in Figure5.

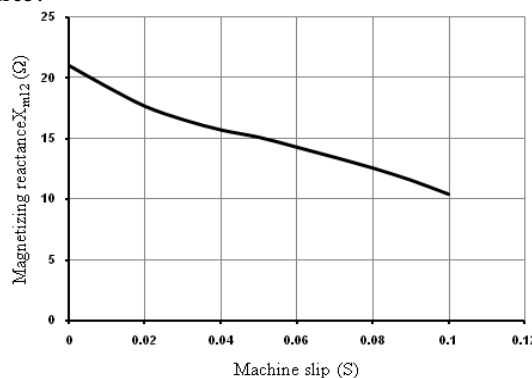


Figure 5. The Linear Magnetizing Reactance Variation against the Machine Slip

5 Case Study and Performance

The proposed model is tested at different load conditions. The load conditions are considered as operation at different wind speed, different load impedances and different values of shunt capacitor. The Induction machine parameters are shown in Table 1.

Table 1. Induction Machine Parameters.

Rated power	175 W
Voltage	206 V
Input current	1.2 A
Frequency	60 Hz
Pole pair	2
Rated speed	1670 r.p.m
Stator resistance	12.675Ω
Rotor resistance	12.675Ω
Stator reactance	12Ω
Rotor reactance	8.4Ω
Mutual reactance	184.5Ω

The following cases show the model performance due to many cases of effects; the magnetizing current variation, efficiency variation, power variation and power factor variation.

5.1 The Magnetizing Current Variation

Figure6(a,b&c) shows the variation of the magnetizing current against the induced air gap voltage at shunt capacitors equal to $25\mu F$, $45 \mu F$ and $65 \mu F$ respectively and wind speed equals to $1p.u$ and $1.05p.u$. The magnetizing current equals to zero when the induced air-gap voltage equals the internal

armature induced voltage E_{pm} . The results given by the model take into consideration the effects of the wind-speed and the shunt capacitance values. The result shows that increasing the value of the shunt capacitance leads to increase in the magnitude of the magnetizing current; however, the increase in the wind-speed lead to decrease in the rate of changing of the magnetizing current with respect to the induced air-gap voltage. Figure 6 shows these results.

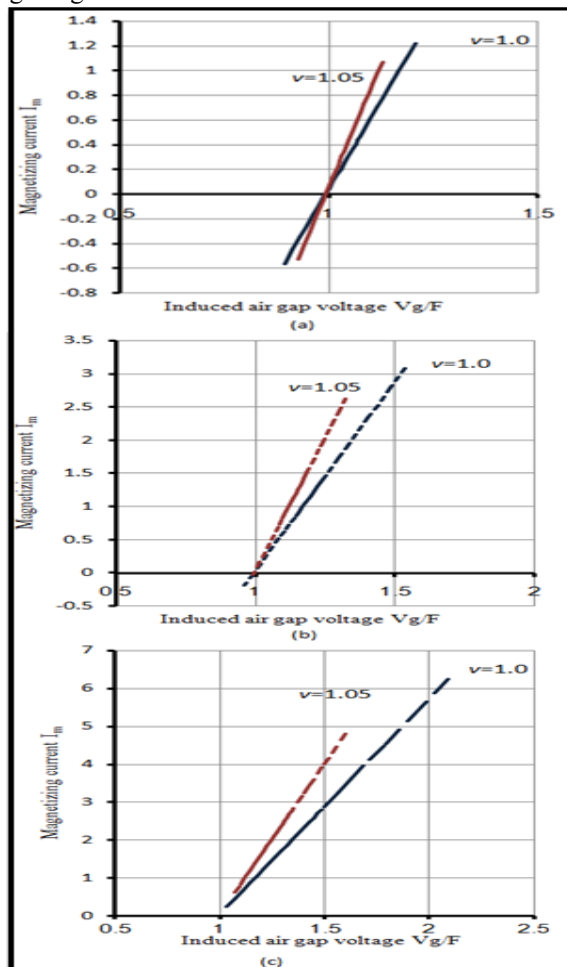


Figure 6. Magnetizing Current Variation against the Induced Air-Gap Voltage at Different Speed And Capacitor Values.

5.2 The Variation of the Nonlinear Magnetizing Reactance

Figure 7 (a) shows the relation between the magnetizing reactance against the internal induced air gap voltage (E_g) given by reference [6], Figure 7(b) shows the relation between the magnetizing reactance against the internal induced air gap voltage (E_g) that obtained from the proposed model of PMSEIG. By comparing the experimental and curve fitting values of Figure 7 (a) [6] with the calculated results obtained by the proposed model plotted in Figure 7 (b), it's clear that there is a fairly agreement with a satisfied accuracy above 91% as shown in Table 2. However, this error 9% is attributed to many reasons such as the error of measuring instruments used in experiment, the error due to the way of computing the results (the proposed iterative solution) and the error due to neglecting the core losses in the proposed model.

Table 2. Magnetizing Reactance Values.

E _{g12}	(V)	10	30	40	50
X _{m12} (Experimental)	(Ω)	8.9	11.8	13.8	14.9
X _{m12} (Predicted)	(Ω)	8.1	11.8	13.5	14.9
% error =	$\frac{X_{m12} \text{ (Experimental)} - X_{m12} \text{ (Predicted)}}{X_{m12} \text{ (Experimental)}} \times 100$	8.9	0	2.1	0

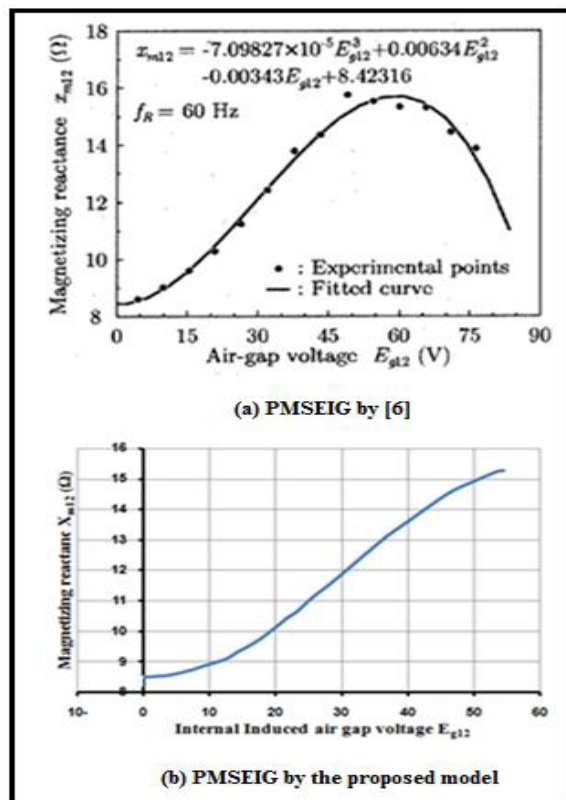


Figure 7. Magnetizing Reactance as A Function of Air-Gap Voltage.

5.3 The Terminal Voltage Variation

The terminal voltage variation against the shunt capacitance values at wind speed $v = 1.05$ p.u. is given by reference [6] in Figure8 (a) while the corresponding results obtained by the proposed model of PMSEIG are shown in Figure8 (b). Both trends show that the terminal voltage is increasing as the shunt capacitance value is increased. Comparing both trends shows that the accuracy of the results obtained by the proposed model is above 94%. Table3 shows the comparison of different shunt capacitance values. The error is limited to 5.5% taking into consideration all the reasons of the error that discussed previously.

Table 3. Terminal Voltage Values at Different Shunt Capacitance.

C (μF)	20	40	60
$V_t(\text{Experimental})$ (V)	64	68	77
$V_t(\text{Predicted})$ (V)	65.9	71.8	81.2
$\% \text{ error} = \frac{V_t(\text{Experimental}) - V_t(\text{Predicted})}{V_t(\text{Experimental})} \times 100$	2.9	5.5	5.5

5.4 Terminal Voltage and Output Frequency Variations Against the Load Current

The corresponding results obtained by the model are given in Figure9 for (R-L) load with 0.7 PF. The figure shows different variation for both the output frequency and the terminal voltage with respect to the load current. The output frequency and terminal voltage decreased with the load current increasing.

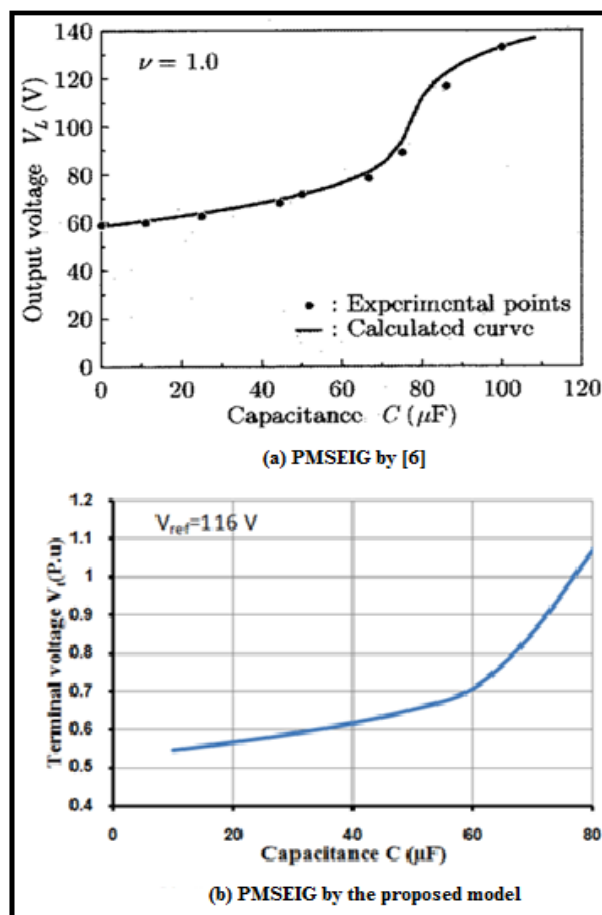


Figure 8. Terminal Voltage Variation Against The Shunt Capacitance

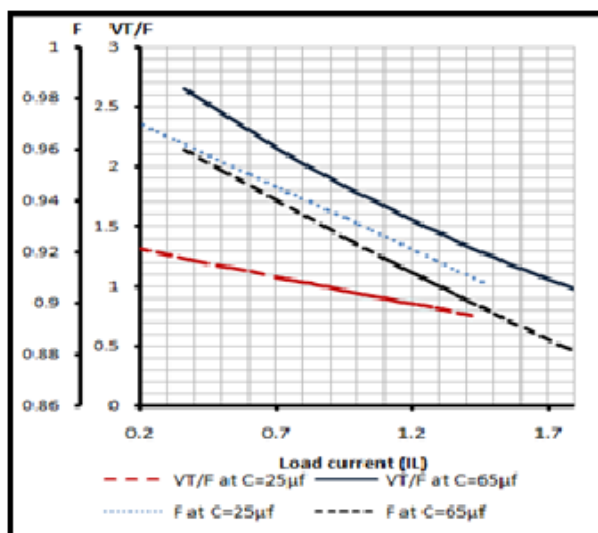


Figure 9. Output Frequency And Terminal Voltage Variation Against The Machine Slip

6 Conclusions

The paper is aimed to present the PMIG as a standalone unit in a wind energy system (PMSEIG) and to develop a simple technique based on iterative solution. From the analysis of the obtained results in this paper, the contributions are summarized as follows:

1. The difficulty of assessing varied value of the magnetizing reactance and variation of both the terminal machine voltage and generated stator frequency with the operating load conditions such as wind-speed, shunt capacitance value, and load impedance has been overcame through the following steps:
 - The equivalent circuit of the PMSEIG its developed in the per-unit stator frequency of the machine
 - The predicted values obtained from iterative solution with prior unknown machine parameters such as the magnetizing reactance, the per-unit stator frequency, and the induced air-gap voltage under a well specified machine load condition are predicted.
 - The full performance of the PMSEIG is solved using the equivalent circuit taking into consideration the obtained predicted values of the circuit parameters.
2. The solution convergence is tested for either resistive loading or resistive-inductive loading condition of 0.7 lagging PF.
3. The accuracy of the proposed iterative solution is satisfied as the results are tested and compared with the trends and results of the corresponding experimental and numerical results published in three different references (where the maximum error of the solution obtained is less than 9% compared to [6]).
4. The discussions of PMSEIG results are concluded and introduced the full performance of the machine taking into the consideration the effects of the machine parameters and loading types.

References

1. Potgieter, J.H.J., Lombard, A.N., Wang, R.J., and Kamper, M.J. , “Evaluation of permanent-magnet excited induction generator for renewable energy applications”, Proceedings of the 18th Southern African Universities Power Engineering Conference, Stellenbosch, South Africa, 299-304, (2009).

2. Sung-Hooii Kiln and Song-yop Hahn" *Analysis and design of a induction generator with a super conducting bulk magnet rotor*", IEEE Transactions on Applied Super conductivity, **Vol. 1**, pp.931-934, March (2000).
3. Fukami, Nakagawa, K., Kanamaru, Y., and Miyamoto, T. "A technique for the steady-state analysis of a grid-Connected permanent-magnet induction generator", IEEE Transactions on Energy Conversion,**Vol.19**, pp. 318-324, June (2004).
4. Troster, E.; Sperling, M.; and, Hartkopf, T.H, "Finite element analysis of a permanent magnet induction machine", Proceeding of International Symposium on Power Electronics, Electrical Drives, Automation and Motion (SPEEDAM), (2006).
5. Tsuada, T., Fukami, T., Kanamaru, Y., and Miyamoto, "Effects of the built-in permanent magnet rotor on the equivalent circuit parameters of a permanent magnet induction generator", Proceeding of IEEE Transaction on Energy Conversion, **Vol. 22**, pp. 798-799 , September (2007).
6. Fukami, Tadashi; Shimizu, Bungo; Hanaoka ,Ryoichi; Takata, Shinzo; Miyamoto, Toshio" Performance prediction of a stand-alone permanent-magnet induction generator" IEEE Transactions on Industry Applications, Volume 123, Issue 7, pp. 817-823 (2004). [7] S.C.Tripathy ,M.Kalantar and N.D.Rao "Wind turbine driven self-excited induction generator" proceeding of Energy Convers.Mgl , **Vol. 34** ,vol8,pp. 641-648,(1993).
7. S.C.Tripathy, M.Kalantar and N.D.Rao "Wind turbine driven self-excited induction generator" Proceeding of Energy Convers.Mgl, **Vol. 34**, pp. 641-648, August (1993).
8. A. Abou,M. Barara, A.Ouchatti,M. Akherraz and H. Mahmoud, "Capacitance required analysis for self excited induction generator" Journal of Theoretical and Applied Information Technology, **Vol. 55** No.3, pp. 382-389, September (2013).